AN INTELLIGENT ACTIVE-PASSIVE VIBRATION ABSORBER USING HIERARCHICAL FUZZY APPROACH

J. Lin

Abstract—**It has been shown that piezoelectric materials can be used as be highly promising for application as passive electromechanical vibration absorbers by shunting them with electrical networks. However, these passive devices have limitations that restrict their practical applications. The main goal of this work is to develop a novel approach for achieving a high performance adaptive piezoelectric absorber – an active-passive hybrid configuration. Owing to the adaptive capability of fuzzy inference systems, its applications to the active control are immediate. This investigation addresses the first application of the concept of hierarchy for controlling fuzzy systems in such an active-passive absorber. One of the main advantages of using a hierarchical fuzzy system is to minimize the size of the rule base by eliminating "the cruse of dimensionality". Although the performance of the optimal passive absorber is already much better than the original system (no absorber), the intelligent active-passive absorber can still outperform the passive system significantly. The fuzzy control method appears quite useful as regards reliability and robustness.**

I. INTRODUCTION

Recent advances in piezoelectric actuators, based on the converse piezoelectric effect, have great potential for the active control of vibrations, especially for suppressing or isolating vibrations [1, 2, 3, 4].

Numerous applications exist in which the addition of passive vibration damping to a structural system can significantly improve system performance or stability. Piezoelectric materials have been shown to have potential as passive electromechanical vibration absorbers by shunting them with electrical networks. By placing electrical impedance across the terminals of the PZT, the passive network is capable of damping structural vibrations. If a simple resistor is placed across the terminals of the PZT, the PZT will act as a viscoelastic damper. If the network consists of a series inductor-resistor *R-L* circuit, the passive network combined with the inherent capacitance of the PZT creates a damped electrical resonance [5]. Passive shunt damping is regarded as a simple, low cost, lightweight and easy to implement method of controlling structural vibrations. A desirable property of passive shunt damping is that the controlled system is guaranteed to be stable in the presence of structural uncertainties.

Flexible mechanical structures have an infinite number of resonant frequencies (or structural modes). If the tuned energy absorber is used to minimize a number of modes, one would need an equal number of PZT patches and shunting circuits. This is clearly impractical.

Recently, the concept of semi-active piezoelectric absorbers has also been proposed to suppress harmonic excitations with time-varying frequencies. Owing to their active and passive damping features, piezoelectric materials have been explored to determine their active-passive hybrid control abilities, which can possess the advantages of both passive and active systems. Hence, reference [6] outlines new insights derived from analyzing the active-passive hybrid piezoelectric network concept (APPN).

However, these semi-active devices have limitations that restrict their practical applications [7]. Therefore, the approach proposing a high performance active-passive alternative to semi-active absorbers is shown in [3]. Furthermore, the effectiveness of this new absorber design is first demonstrated through experimental investigations and indicated in [4].

The above literature review has not identified any examples of the application of the fuzzy control theory in active-passive vibration absorber using a hierarchical concept. Consequently, this study develops a novel approach for achieving a high performance adaptive piezoelectric absorber – an active-passive hybrid configuration.

II. MODELING THE COMPOUND SYSTEM

Figure 1 schematically illustrates the proposed system, which consists of a piezoelectric actuator integrated with an active voltage source in series with an *RL* circuit. The elastic deflection of a beam is described by:

$$\frac{\partial^2}{\partial x^2}\left[EI\frac{\partial^2 y(x,t)}{\partial x^2} - C_a v_a(x,t)\right] + \rho A_b \frac{\partial^2 y(x,t)}{\partial t^2} = 0, \quad (1)$$

where E, I, A_b, and ρ represent the Young's modulus, moment of inertia, cross-sectional area, and linear mass density of the beam, respectively. Moreover, the parameter C_a is a constant dependent on the actuator properties.

Using the modal analysis techniques, the position function $y(x,t)$, can be expanded as an infinite series of the form[8, 9]:

Manuscript submitted September 11, 2004. This work was supported in part by the National Science Council of the Republic of China, Taiwan under Contract No. NSC 92-2213-E-231-002.

J. Lin was with the Department of Mechanical Engineering, Ching Yun University, 229, Chien-Hsin Rd., Jung-Li, Taiwan 320, R.O.C. (e-mail: jlin@cyu.edu.tw).

$$y(x,t)=\sum_{i=1}^{\infty}\phi_i(x)q_i(t)\,, \tag{2}$$

This study assumes that the model of the structure and the piezoelectric absorber can be obtained in Eq. (3) [5]:

$$\begin{aligned} &M\ddot{q}+C\dot{q}+Kq+K_cQ_p=\hat{F}\cdot f(t)\\ &L_p\ddot{Q}_p+R_p\dot{Q}_p+\frac{1}{C_p^s}Q_p+K_c^Tq=V_c \end{aligned}\,. \tag{3}$$

Moreover, the L_p and R_p are the passive inductance and resistance of the shunt circuit, Q_p denotes the charge on the piezoelectric, C_p^s represents the capacitance of the piezoelectric under constant strain, and V_c is the control voltage.

Furthermore, C_p^s and K_c^T can be defined as [6]:

$$C_p^s=\frac{b_s(x_2-x_1)}{\beta_{33}(h_s-h_b)}\,, \tag{4}$$

$$K_c^T=\frac{h_{31}(h_s^2-h_b^2)}{2(x_2-x_1)}[\phi'(x_2)-\phi'(x_1)]\,. \tag{5}$$

where b_s denotes the width of the beam and PZT, h_b represents the distance from the beam neutral axis to the outside surface of the beam, and h_s is the distance from the beam neutral axis to the outside surface of the PZT. Additionally, (x_2-x_1) is the length of the PZT, h_{31} denotes the piezoelectric constant and β_{33} represents the dielectric constant of PZT.

Hence, the system be expressed in the following form:

$$\dot{x}=A(R_p,L_p)x+B_1\hat{f}+B_2(R_p,L_p)u\,. \tag{6}$$

where x denotes the state vector, u is the control input, $\hat{f}$ represents the external disturbance vector. The system matrix, A, and the control matrix, B_2, are functions of the passive resistance and inductance.

This study defined,

$$x=\begin{bmatrix} q & Q_p & \dot{q} & \dot{Q}_p \end{bmatrix}^T;$$

$$A=\begin{bmatrix} 0 & 0 & 1 & 0\\ 0 & 0 & 0 & 1\\ -M^{-1}K & -M^{-1}K_c & -M^{-1}C & 0\\ -K_c^T/L_p & -C_p^s/L_p & 0 & -R_p/L_p \end{bmatrix};$$

$$B_1=\begin{bmatrix} 0 & 0 & M^{-1}\hat{F} & 0 \end{bmatrix}^T;$$

$$B_1=\begin{bmatrix} 0 & 0 & 0 & 1/L_p \end{bmatrix}^T.$$

The system described above has (n+1) modes. The (n+1)th mode is due to the passive circuit. Importantly, the addition of an active absorber of this type to a principal system results in a combined system with an added degree of freedom. Because the comparison functions in the expansion are chosen to be the eigenfunctions of a cantilever beam, the ith generalized coordinate closely resembles the ith structural modal coordinate (i=1, 2, 3, … , n). Moreover, for obvious reasons the infinite-order model produced by the model analysis techniques is not suitable for use in the optimization. Consequently, to perform the optimization, an accurate model of the system is required. The following section proposes an optimization approach for determining appropriate values for the shunt circuit.

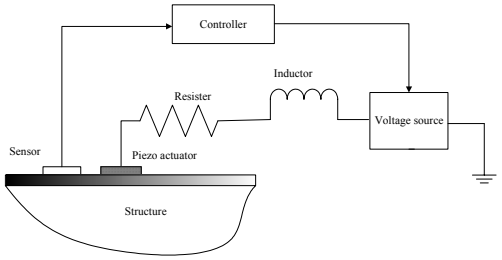

FIG. 1 ADAPTIVE STRUCTURE WITH ACTIVE-PASSIVE HYBRID PIEZOELECTRIC NETWORKS

III. DETERMINING THE SHUNTING CIRCUIT VIA OPTIMIZATION

The form for the passive damping can express as:

$$\dot{x}=A(R_p,L_p)x+B_1\hat{f}\,, \tag{7}$$

Here, the control action u is not included since this system is a passive system. Thus, this study assumes that $\hat{f}(t)$ is given by

$$\hat{f}(t)=D_d(t)x_d(t)\,. \tag{8}$$

Here $x_d(t)$ is the solution of

$$\dot{x}_d(t)=A_d(t)x_d(t)+B_d w(t)\,, \tag{9}$$

where $w(t)$ is white noise. This work further assumes that both $x(t_0)$ and $x_d(t_0)$ are stochastic variables. Moreover, the mean and spectral density of $w(t)$ are given by $E[w(t)]=0$ and $E[w(t)w^{\mathrm{T}}(\tau)]=V(t)\delta(t-\tau)$; $E[\ ]$ is the expectation operator.

Therefore, ate vector, and the overall system become

$$\dot{\tilde{x}}=\begin{bmatrix} A(t) & D_d(t)\\ 0 & A_d(t) \end{bmatrix}\tilde{x}+\begin{bmatrix} 0\\ B_d \end{bmatrix}w(t)=A_a\tilde{x}+B_a w(t)\,. \tag{10}$$

where $\tilde{x}(t)=\begin{bmatrix} x(t) & x_d(t) \end{bmatrix}^{\mathrm{T}}$.

The deterministic regulator problem considered the cost function

$$J_t=\lim_{t\to\infty}E[\tilde{x}^{\mathrm{T}}Q\tilde{x}]\,, \tag{11}$$

where Q represents a nonnegative definite weighting matrix. Here, $\tilde{x}^{\mathrm{T}}Q\tilde{x}$ represents the overall structure energy.

Moreover, the system response consists of a state vector with zero mean and a variance given by the solution ($\tilde{P}$) to the Lyapunov function

$$A_a^T\tilde{P}+\tilde{P}A_a+Q=0\,. \tag{12}$$

This equation leads to the following constrained optimization problem:

$$\mathrm{R}^*=\arg\min_{\text{s.t. g=0}}J\,, \tag{13}$$

where $g = A_a^T \widetilde{P} + \widetilde{P} A_a + Q$.

With a given set of passive parameters (R and L), the cost function L is

$$L = tr(B_a D_d B_a^{\mathrm{T}} \widetilde{P}) . \quad (14)$$

Notably, for each set of the passive control parameters R and L, there exists an optimal control with a corresponding minimized cost function. A sequential quadratic programming algorithm [10] can be used to determine the resistance and inductance that further minimize J.

IV. ACTIVE-PASSIVE CONTROL LAW DESIGN

However, passive control is economical but can only control the vibration up to a certain limit. On the other hand, an active control operates with external energy continuously supplied. Restated, this study is applying active control on an optimized (tuned circuit) passive system.

4.1 Analysis of Hierarchical Fuzzy System

Equation (2) shows that the beam vibration system is an infinite series form. Additionally, while the large-scale system has been to the reduced-order truncated system Through this process, by virtue of linearization, delay approximation, decomposition, and model reduction, each step and/or assumption has introduced a degree of uncertainty into the system, moving the model away from the true physical situation. The above discussion brings up another point, namely that frequent, simplifying assumptions make the problem at hand too uncertain to be of practical use. The design and analysis of a large-scale system should be based on the best available knowledge instead of the simplest available model to treat system uncertainties. Therefore, a large-scale system is better treated via knowledge-based methods such as fuzzy logic, neural networks, etc [11].

The design of fuzzy controllers is often a time-consuming activity that depends on knowledge acquisition, the definition of the controller structure, and the definition of rules and other parameters. Currently, an important issue related to fuzzy logic systems is the reduction of the total number of rules and their corresponding computational demands.

Furthermore, the computational complexity in the process can be reduced as a consequence of the rule-base size reduction, which has become one of the main concerns among system designers. As the application domain of fuzzy control expands from simple systems to more complex systems, a serious limit on the standard fuzzy controller arises as the number of rules in a standard fuzzy controller increases exponentially with the number of variables involved. Given n variables and m fuzzy sets defined for each variable, m^n rules are required to generate a complete fuzzy controller. As n increases, the rule base quickly overloads the memory and makes the fuzzy controller rather difficult to implement. The concept of the "hierarchical rule set" is elucidated to overcome this problem. Given this hierarchical structure, the number of rules increases linearly (not exponentially) with the number of system variables [11, 12].

Furthermore, a hierarchical fuzzy control structure is used, where the most influential parameters are chosen as the system variables in the first level, the next most important parameters are selected as the system variables in the second level, and so on. For various practical problems, it may be known that some variables are more important than others.

Hierarchical fuzzy control contains several level rule sets. The first level rule set gives a basic control action, while the higher level rule sets initiate fine tuning control action based on the base (gross) control action. Generally, the first level rule set depends upon only a few important system variables, while the higher-level rule sets rely on a larger number of system variables. Each controller aims at the global behavior of the reference FLC, regardless of the missing information regarding the other inputs. To avoid initiating an undesirable control action, the final control action should mainly depend on the first level rule set in the event of system parameter perturbation. Furthermore, for such a fuzzy system illustrated in Fig. 2, with four variables and seven fuzzy sets (labels), the number of rules is reduced from $7^4 = 2401$ to $7^2 + 7^2 + 7^2 = 147$, indicating a 93.88% reduction. Clearly, depending how many flexible modes can be fused and in what order, when these modes are put into a hierarchical structure, the size of the rule base is reduced differently.

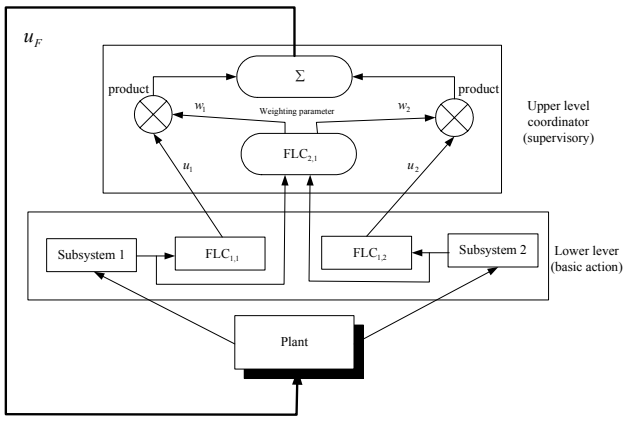

Fig. 2 Implementation of Hierarchical Fuzzy Controller

4.2 Fuzzy Control Structure of the System

The design of the local controllers takes into account each subsystem ignoring the interactions among them, while a higher-level controller handles subsystem interactions. Figure 2 illustrates the employment of the hierarchical technique for the system.

For such a case, the hierarchical fuzzy controller suppresses the vibrations in a flexible structure using piezoelectric actuators. Typically, the response of a beam is dominated by the lower (1st, 2nd, 3rd…) modes. Consequently,

few flexible retained modes are selected for the system in an approximate dynamic model.

To implement the proposed technique, the system is decomposed into two subsystems: the first subsystem takes q_{f1} and $\dot{q}_{f1}$ as local variables, while the second subsystem takes q_{f2} and $\dot{q}_{f2}$ as local variables. Hence, in the proposed hierarchical fuzzy control structure, the first subsystem rules are those associated with the first flexible mode, and its derivatives are used to generate the first-level hierarchy. The second most dominant mode and its derivative are selected as inputs to another fuzzy controller at the same level, and so on.

The fuzzy logic controller FLC_1 takes q_{f1} and $\dot{q}_{f1}$ as inputs to generate the local control action u_1 while fuzzy logic controller FLC_2 takes q_{f2} and $\dot{q}_{f2}$ to generate another control action u_2. Thus, at the local level, each subsystem is designed separately. The fuzzy logic rule base for each subsystem is designed based on the dynamic response of each mode when a control force is activated on the flexible system.

At the upper level, the information from each subsystem is taken as an input to the coordinator. To coordinate the local subsystems, the upper level FLC takes $q_{f1} - q_{f2}$ and $\dot{q}_{f1} - \dot{q}_{f2}$ as inputs to generate the weighting functions w_1 and w_2. Hence, the upper level controller monitors these differences and causes the supervisory decision to be fed to the lower level. The weight factors w_1 and w_2 generated by the supervisory fuzzy logic controller are multiplied with the local controls u_1 and u_2. These are then summed to form the total control u_F for feeding back to the flexible beam. Furthermore, the weighting factor (output scaling factor) is self-regulated during the control process, and can optimize the gain for the hierarchical fuzzy controller.

However, fuzzy logic may be best used to implement high-level or supervisory functions in a hierarchically structured intelligent control system. As depicted in Fig. 2, fuzzy logic control can appear at the higher levels, and acts as the supervisory control or coordinator. Fuzzy logic offers a twofold advantage in this setting. First, fuzzy logic can facilitate the synthesis of supervisory control strategies due partly to its ability to better represent the semantics of linguistic terms and constructs often used in supervisory control strategies.

Second, because fuzzy logic-based control strategies can be viewed as nonlinear control strategies, analytical study of the resulting hierarchical system can be facilitated.

4.3 Fuzzy Logic Controller Design

1) Define Input and Output Variables, Fuzzy Partition, and Builds the Membership Functions

Error and error change are two commonly used variables in fuzzy control. This study uses the vibration states and their rate variables as inputs, with the voltage applied to the voltage amplifier as the output. Since the fuzzy inference system handles smooth membership functions better than trapezoidal ones in vibration control, bell-shaped functions are employed to convert these inputs and output variables into linguistic control variables.

The rule base design of two subsystems is based on pre-simulation investigations. Fuzzy quantities such as *large negative* (LN), *medium negative* (MN), *small negative* (SN), *zero* (ZE), *small positive* (SP), *medium positive* (MP), *large positive* (LP), and so on, are used in the statements, and the corresponding membership functions thus are needed. Moreover, in building the supervisory rule set, the knowledge of on tuning weighting factor, gained from the experience (or knowledge) of tuning the fuzzy logic controller, is used and stated as a set of linguistic statements. The viewer surface for the weighting factor is presented in Fig. 3. Moreover, Fig. 4 displays the rule view of the upper level coordinator.

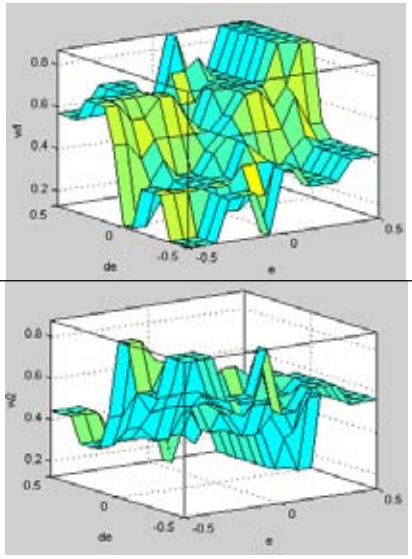

Fig. 3 The viewer surface for the weighting factor w_1, w_2

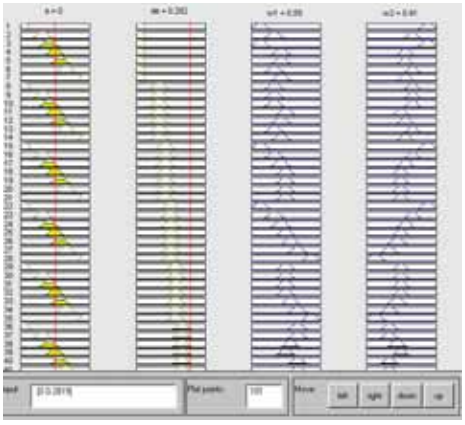

Fig. 4 Rule view of the upper level coordinator

2) Composite Control of the system

A hierarchical fuzzy approach is pursued which allows the adaptation of a composite control strategy. The total (final) control action of the hierarchical fuzzy controller (Fig.

2) is composed of the control actions due to different level rule sets; that is

$$u_F = \sum_{i=1}^{2} w_i u_i \ , \tag{15}$$

where u_F represents the final control action; u_i is the control action obtained by consulting the *i*th fuzzy rule set, and w_i is the corresponding weighting factor.

V. EXPERIMENTAL IMPLEMENTATION

An experimental apparatus was constructed, and it is constituted by a flexible cantilever aluminum beam type structure with piezoelectric patches symmetrically bonded on both sides to provide structural bending. Figure 5 schematically depicts the control experiment. A strip-bender type BM500/120/6 piezoelectric actuator and strain gauge are attached to the surface of the beam to serve as an actuator and sensor, respectively. Because the PZT effect is a dual effect, bending elements are successfully used as vibration and force sensors as well as small electrical generators. The piezoactuator is connected to an *R-L* circuit as well as an active voltage source.

VI. RESULTS AND DISCUSSION

The beam consists of a 15-cm long uniform and a rectangular cross section 19mm × 3mm with fixed-free conditions..

Case 1. Frequency Responses

For the system described in the previous section, the overall structural response is a sum of the response contributed from the excitation force $\hat{f}$ and that contributed from the control voltage V_c. Figure 6 plots the measured midpoint deflection of the beam and the step excitation frequency responses. It compares the peak magnitude with and without the shunt circuit. The resonant responses of the first two modes are reduced considerably once the shunt circuit is introduced. That is, the *RL* circuit enhances the passive damping ability around the first resonant frequency. Moreover, the frequency response of the controller is illustrated in Figs. 7 and 8. The frequency response under passive damping (open-loop) and the control of the hierarchical fuzzy logic (closed-loop) are presented, respectively. The controller is observed to have a resonant structure, as expected. Moreover, the resonant response of the first two modes reduces over the entire beam due to the controller action. Table 1 lists the magnitude reduction at the first resonance frequency for each specified *RL* circuit of the beam vibration. The table also lists the magnitude reduction, such as the shift in the first resonant frequencies of the beam vibration. The experiments demonstrate that the resonant responses (711.5 rad/s) of the first mode have been reduced by around 11.26 dB to 30.85 dB when the shunt circuit is applied. Furthermore, compared to passive damping, the first modal resonant magnitudes are reduced by up to 66.63 db while the active controller undertaking. Notably, the reduction in peak vibration amplitude is greater for the active-passive absorber than for passive damping such as the shift in resonant frequencies. Hence, the controller reduces the resonant responses of the structure by increasing the system damping at resonant frequencies. Moreover, as can be seen, the system sensitivities to the active controller are exceeding those for passive damping. As the resonant frequency reduces, the magnitude reduction increases In contrast, the magnitude reduction decreases with increasing resonant frequency.

Case 2. Time Responses

Figures 9 and 10 plot the time response for vibrational displacement at the midpoint of a beam under an initial excitation step for various resistance and inductance values. These indicate the effectiveness of the hierarchical fuzzy controller in minimizing structural vibration in the time domain. The settling time of the position response has been reduced considerably by the fuzzy control action. Additionally, Figs. 9 and 10 also show the effectiveness of the controller effectiveness in minimizing beam vibration in the time domain. Furthermore, Table 2 lists the normalized Root-Mean-Square (RMS) vibrational displacement at the midpoint of a beam under uncontrolled, passive, and active-passive absorber for various resistance and inductance values. Evidently, a vibration reduction (%) for passive absorber is highly dependent upon the resistance and inductance values with the shunt circuit. Moreover, a hierarchical fuzzy controller yields a more significant improvement in displacement reduction over that obtained by LQR techniques. Table 2 also reveals that the proposed passive absorber reduces the displacement due to vibration of an uncontrolled by approximately 8.7% ~ 54.37% at each specified *RL* circuit. Moreover, once again the performance of the intelligent active-passive absorber is relatively unaffected by the change in the shunt circuit parameters. The normalized RMS is around 1.2e-4 to 1.7e-4 by implementing the intelligent active-passive absorber. Compared with the system with no absorber, the performance of the intelligent active-passive absorber is considerably better than that of the passive damping in vibration reduction.

REFERENCES

[1] W. Chang, S.V. Gopinathan, V.V. Varadan, and V.K. Varadan, "Design of robust vibration controller for a smart panel using finite element model," *Trans. of the ASME J. of Vibration and Acoustics*, vol. 124, pp. 265-276, 2002.

[2] D. Halim and S.O. Reza Moheimani, "Spatial resonant control of flexible structures – application to a piezoelectric laminated beam," *IEEE Trans. on Control System Technology*, vol. 9, no. 1, pp. 37-53, 2001.

[3] R.A. Morgan and K.W. Wang, "An active-passive piezoelectric absorber for structural vibration control under harmonic excitations with time-varying frequency, part 1: algorithm development and analysis," *Trans. of the ASME J. of Vibration and Acoustics*, vol. 124, pp. 77-83, 2002.

[4] R.A. Morgan and K.W. Wang, "An active-passive piezoelectric absorber for structural vibration control under harmonic excitations with time-varying frequency, part 2: experimental validation and parametric study," *Trans. of the ASME J. of Vibration and Acoustics*, vol. 124, pp. 84-89, 2002.

[5] N.W. Hagood and A. von Flotow, "Damping of structural vibrations with piezoelectric materials and passive electrical networks," *Journal of Sound and Vibration*, vol. 146, no. 2, pp. 243-268, 1991.

[6] M.S. Tsai and K.W. Wang, "On the structural damping characteristics of active piezoelectric actuators with passive shunt", *Journal of Sound and Vibration*, vol. 221, no. 1, pp. 1-22, 1999.

[7] C.L. Davis and G.A. Lesieutre, "An actively tuned solid-state vibration absorber using capacitive shunting of piezoelectric stiffness", *Journal of Sound and Vibration*, vol. 232, no. 3, pp. 601-617, 2000.

[8] J. Lin and F.L. Lewis, "Two-time scale fuzzy logic controller of flexible link robot arm", *Fuzzy Sets and Systems*, vol. 139, no. 1, pp. 125-149, 2003.

[9] J. Lin, "A hierarchical fuzzy logic controller for flexible link robot arms during constrained motion tasks", *IEE Proceedings – Control Theory and Applications*, vol. 150, no. 4, pp. 355-364, 2003.

[10] F.L. Lewis, *Applied Optimal Control & Estimation-Digital Design & Implementation*, Prentice Hall, Englewood Cliffs, NJ, 1992.

[11] Jamshidi, M.: *Large-Scale Systems: Modeling, Control, and Fuzzy Logic*, Prentice Hall, 1996.

[12] L.-X. Wang, "Analysis and Design of hierarchical fuzzy systems", *IEEE Trans. on Fuzzy Systems*, vol. 7, no. 5, pp. 617-624, 1999.

Fig. 5 Experimental apparatus

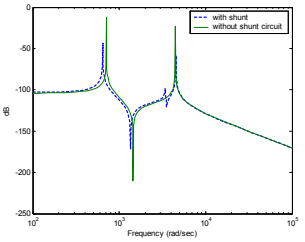

Fig. 6(2500Ω ×79H)

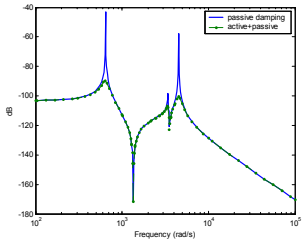

Fig. 7 (5000Ω ×79H)

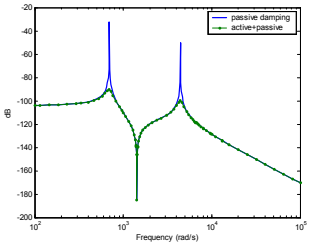

Fig. 8 (5000Ω ×22H)

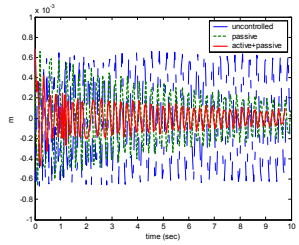

Fig. 9 (2500Ω ×79H)

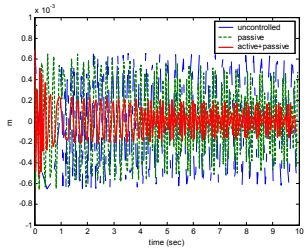

Fig. 10 (2500Ω ×22H)

Table 1 Magnitude reduction at the first resonant frequency

	Reduction 1 (711.5 rad/s)	Reduction 2 (711.5 rad/s)	Reduction 1 (259.4 rad/s)	Reduction 2 (259.4 rad/s)	Reduction 1 (850.4 rad/s)	Reduction 2 (850.4 rad/s)
1500Ω ×22H	11.26 dB	66.63 dB	11.18 dB	74.76 dB	11.33 dB	65.07 dB
2500Ω ×22H	14.7 dB	63.2 dB	14.62 dB	71.32 dB	14.75 dB	61.63 dB
5000Ω ×22H	19.89 dB	58.01 dB	19.80 dB	66.14 dB	19.96 dB	56.44 dB
1500Ω ×79H	20.94 dB	56.48 dB	20.17 dB	63.78 dB	21.20 dB	54.82 dB
2500Ω ×79H	25.07 dB	52.36 dB	24.29 dB	59.65 dB	25.33 dB	50.68 dB
5000Ω ×79H	30.85 dB	46.85 dB	30.07 dB	53.87 dB	31.12 dB	44.91 dB

Note: Reduction 1: (Uncontrolled)-(Passive); Reduction 2: (Passive)-(Active+Passive)

Table 2 Normalized RMS vibrational displacements at the midpoint of a beam

	Uncontrolled (I)	Passive (II)	Active+ Passive (III) (LQR)	Active+ Passive (IV) (fuzzy)	Reduction (%) (I-II)/I	Reduction (%) (I-IV)/I	Reduction (%) (II-IV)/II
1500Ω ×22H	4.6e-4	4.2e-4	3.0e-4	1.7e-4	8.7%	63.0%	59.5%
2500Ω ×22H	4.6e-4	4.0e-4	2.8e-4	1.6e-4	13%	65.2%	60.0%
5000Ω ×22H	4.6e-4	3.5e-4	2.7e-4	1.5e-4	23.9%	67.4%	57.1%
1500Ω ×79H	4.6e-4	3.3e-4	2.5e-4	1.5e-4	28.3%	67.4%	54.5%
2500Ω ×79H	4.6e-4	2.8e-4	2.2e-4	1.4e-4	39.1%	69.6%	50.0%
5000Ω ×79H	4.6e-4	2.1e-4	2.0e-4	1.2e-4	54.3%	73.9%	42.9%